THE JOURNAL OF PHYSICAL CHEMISTRY B

Article

pubs.acs.org/JPCB

Solvent Interactions Stabilize the Polyproline II Conformation of Glycosylated Oligoprolines

Emmanuel B. Naziga,[†] Frank Schweizer,[‡] and Stacey D. Wetmore*,[†]

[†]Department of Chemistry and Biochemistry, University of Lethbridge, 4401 University Drive West, Lethbridge, Alberta, Canada T1K 3M4

[‡]Department of Chemistry, University of Manitoba, 144 Dysart Road, Winnipeg, Manitoba, Canada R3T 2N2

Supporting Information

ABSTRACT: In nature, proline residues carry several post-translational modifications (PTMs), including 4*R* hydroxylation and glycosylation. A recent study synthesized contiguously hydroxylated and glycosylated nonaproline peptides and revealed that both PTMs lead to a significant increase in the thermal stability of PPII relative to the unmodified oligoproline. The increased stability of the hydroxylated peptide can be explained by increased stability of the *trans* isomer due to stereoelectronic effects. However, the effects of glycosylation cannot be completely explained by stereoelectronics since previous experimental results indicate that 4*R*-glycosylation does not produce observable changes in the *trans* preference compared to 4*R*-hydroxylation. We therefore used sophisticated molecular modeling techniques to determine the reason for the further increase in thermal stability upon glycosylation. Free energy estimates obtained from adaptively biased molecular dynamics calculations in implicit (explicit) solvent are −9 kcal mol^{-1} (−20 kcal mol^{-1}) for the hydroxylated compound and −9 kcal mol^{-1} (−46 kcal mol^{-1}) for the glycosylated compound, indicating that direct solvent−peptide interactions are vital for explaining the glycosylation effects on PPII stability. Our data reveals for the first time that interactions between the hydroxyl groups in the glycosylated compound and water act in a complementary fashion with stereoelectronic effects to stabilize the PPII conformation in these substituted oligoproline peptides.

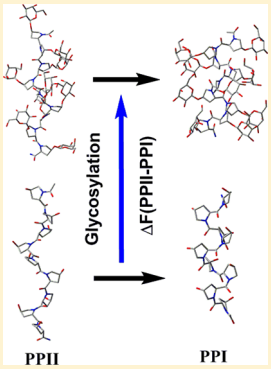

INTRODUCTION

Proline (Pro) differs from other amino acids since its side chain is fused into the backbone. The resulting cyclic backbone leads to conformational rigidity, with the ϕ dihedral angle (Figure 1)

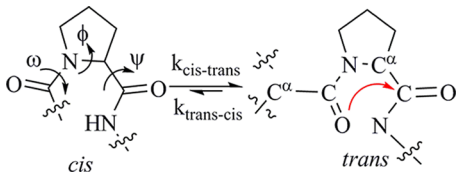

Figure 1. Proline *cis* (ω = 0°) and *trans* (ω = 180°) isomers depicting relevant backbone torsional angles. The ($n \rightarrow \pi^*$) interaction is shown with a red arrow.

restricted to approximately −75°. As a consequence, there is a relatively small energy difference between the Pro *cis* and *trans* isomers (ω, Figure 1), which gives rise to two interesting conformations of the polyproline helices that are characteristic of oligoproline peptides. In particular, the polyproline I conformation (PPI) contains all-*cis* ω bonds and (ϕ, ψ) ≈ (−75°, 160°) (Figure 2), while the polyproline II (PPII) conformation contains all-*trans* bonds and (ϕ, ψ) ≈ (−75°, 145°).

The PPII conformation has become recognized as an important secondary structural motif alongside α helices (e.g., the α_R-conformation with (ϕ, ψ) ≈ (−60°, −50°)) and β-strands (with (ϕ, ψ) ≈ (−120°, 120°)).[1] In particular, PPII is considered to be a significant feature of disordered proteins.[2] Additionally, protein segments that adopt the PPII conformation are important in many biological processes including signaling, cellular mobility and immune response.[3−5] Collagen, which is the most abundant protein in animals, is also dependent on the PPII structure for its characteristic triple helix.[6] Furthermore, hydroxyproline-rich glycoproteins (HRGPs), which are a major component of plant cell walls and are important in several aspects of plant life including growth, embryonic development and defense,[7−9] contain a significant number of (hydroxy) proline residues and adopt the PPII conformation.[10]

The proline residues in collagen (animals) and HRGPs (plants) undergo extensive post-translational modifications (PTMs). Interestingly, many prolines in HRGPs are glycosylated via O-linkages to galactose or arabinose sugars,[7] while this modification has not been observed in animals. Protein glycosylation has been implicated in several functions including enhancing thermal stability, protection from proteolytic degradation and increasing solubility.[11−15] However, a complete understanding of the structure−function relationship of glycosylation has not been achieved. Therefore, studies that

Received: December 18, 2012
Revised: January 25, 2013
Published: January 30, 2013

   dx.doi.org/10.1021/jp312487v | *J. Phys. Chem. B* 2013, 117, 2671−2681

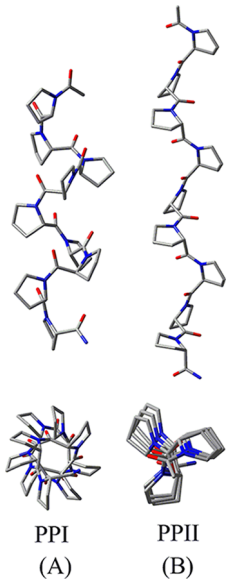

Figure 2. Side (top) and top (bottom) views of helical structures of a polyproline peptide in the (A) PPI and (B) PPII conformations (minimized with AMBER/GLYCAM force field).

provide insights into the direct structural effects of proline glycosylation are necessary.

Although previous studies have examined the effects of several modifications (including fluorination and alkylation) on the properties of a monomeric proline residue,[16−22] only recently was glycosylation considered.[23−27] Experimental data on monomeric models of (4*R*/*S*) hydroxylated proline (hydroxyproline or Hyp) and their glycosylated variants revealed that (*α*/*β*) galactosylation does not provide a detectable increase in the *trans* isomer population of the 4*R* stereoisomer of Hyp.[24] However, a slight stabilization of the *trans* conformation, as well as an increase in the isomerization rate, was observed in the 4*S*-stereoisomer. Nevertheless, both Hyp and the (*α*/*β*) glycosylated peptides favor the *trans* isomer more than unmodified proline. A follow-up computational study revealed that an intramolecular hydrogen bond between a sugar hydroxyl group and the peptide backbone carbonyl, which is sometimes mediated by water, is likely responsible for the observed dependence of the effect of glycosylation on stereochemistry.[27]

Many experimental and computational studies have examined the structure and energetics of oligoprolines.[18,20,21,28−30] For instance, Horng and Raines synthesized oligomers derived from proline, (2*S*, 4*R*)-hydroxyproline, (2*S*, 4*R*)-flouroproline (Flp) and (2*S*, 4*S*)-flouroproline (flp).[18] On the basis of melting temperatures (T_m), stereoelectronic effects ($n \rightarrow \pi^*$, Figure 1) were argued to be responsible for the relative PPII stability of these models, where 4*R* (4*S*) substituents increase (decrease) the PPII stability relative to Pro. A subsequent study by Kuemin et al. of (4*R*/*S*) azidoproline oligomers revealed similar stereoelectronic effects.[20,21] Despite useful information about substituent electrostatic effects, these studies did not consider the effect of glycosylation on the PPII structure.

To obtain quantitative information about the effects of glycosylation on the PPII helix, Schweizer and co-workers recently synthesized Ac−$(Pro)_9$−NH_2 ($(Pro)_9$), Ac−$(Hyp)_9$−NH_2 ($(Hyp)_9$) and Ac−[Hyp−(*β*-D-galactose)]$_9$−NH_2 ([Hyp−(*β*-Gal)]$_9$) model compounds (Figures 3 and S1 (Supporting Information)).[31] Circular dichroism (CD) yielded

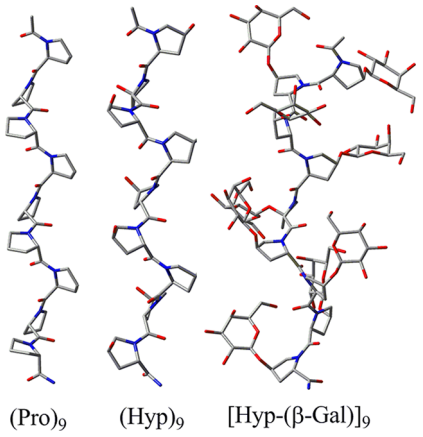

Figure 3. PPII structure of the Ac−$(Pro)_9$−NH_2, Ac−$(Hyp)_9$−NH_2, and Ac−[Hyp−(*β*-D-galactose)]$_9$−NH_2 peptides considered in this study (minimized with AMBER/GLYCAM force field).

T_m estimates of 22 °C, 38 and 70 °C, respectively, which indicates that glycosylation significantly increases the stability of the PPII conformation. Although the increased stability of the *trans* isomer due to hydroxylation explains the T_m difference between $(Pro)_9$ and $(Hyp)_9$, the reason for the increased stability of the PPII conformation in the glycosylated peptide is not clear. Preliminary molecular mechanics minimizations in implicit solvent identified several inter-glycan or glycan−peptide hydrogen bonds in the glycosylated peptide, which may be responsible for the changes in the melting temperatures upon glycosylation.[31] However, other proposals for possible modes of action of a covalently linked sugar have been put forth in the literature, including intramolecular interactions, sterics and (direct or indirect) solvent−sugar interactions.[32−35]

It is clear from the above discussion that more detailed information is needed about how glycosylation affects the PPII structure of oligoprolines and leads to the observed relative thermal stabilities of the unglycosylated and glycosylated oligomers. Therefore, the present work uses a variety of sophisticated molecular modeling methods to provide detailed molecular level analysis on the structure of the galactosylated oligopeptide that both complements and explains experimental observations. Specifically, we initially consider the three model peptides examined by Schweizer and co-workers (Figure 3) using conventional molecular dynamics (MD) simulations. Subsequently, several advanced techniques and extensive sampling procedures, such as replica exchange MD (REMD), adaptively biased MD (ABMD), and a combined Hamiltonian and temperature REMD (HT-REMD), are used to obtain free energy estimates of the PPII to PPI transition. In contrast to previous proposals, our data reveals for the first time that interactions between the hydroxyl groups in hydroxylated or glycosylated compounds and solvent water molecules act in a complementary fashion with stereoelectronic effects to stabilize the PPII conformation in these substituted oligoproline peptides.

METHODS

A thorough conformational analysis of the $(Pro)_9$, $(Hyp)_9$, and [Hyp−(*β*-Gal)]$_9$ peptides must investigate all available degrees of freedom. In particular, the puckering transitions of the Pro ring and variations in the backbone dihedral angles (*ϕ*, *ψ* and *ω*, Figure 1) should be considered. There are two major puckering states in Pro (C^γ−*exo* and C^γ−*endo*), which have

dx.doi.org/10.1021/jp312487v | J. Phys. Chem. B 2013, 117, 2671−2681

been demonstrated by theoretical studies to be well sampled over the course of a standard MD simulation.[36,37] As mentioned in the Introduction, the ϕ ($\angle$(C−N−C^{α}−C), Figure 1) angle in Pro is restricted by the ring system to occupy a narrow band around −75°. While the ψ ($\angle$(N−C^{α}−C−N), Figure 1) dihedral angle is more flexible, it can also be adequately sampled in MD simulations.[38] Thus, the main consideration when designing a sampling protocol for (substituted) oligoprolines is the ω ($\angle$(C^{α}−C−N− C^{α}), Figure 1) dihedral angle, which dictates whether a particular residue adopts the *cis* or *trans* conformation. While the *cis* and *trans* structures of Pro are very close in energy, inter-conversion between these states requires more than 10 kcal/mol of energy.[39−41] Therefore, such conformational changes are not readily observed in a standard MD simulation of several hundred nanoseconds for these types of systems. In addition to the challenges associated with sampling ω, solvent effects must be carefully taken into consideration when studying oligoprolines. Unlike other secondary structural motifs, such as α-helices, the PPI and PPII structures of (unsubstituted) oligoprolines do not afford intramolecular hydrogen bonding. Therefore, interactions with solvent is essential for determining structural preferences.

With the above considerations in mind, we have designed a series of MD simulations that adequately sample all low vibrational modes of the oligopeptides. All calculations were carried out using AMBER 10[42] or 11[43] with the AMBER FF99SB[44] and GLYCAM 06f[45] force fields describing the peptide and sugar moieties, respectively. Additional parameters for the hydroxyproline residue were obtained from Park et al.,[37] and the glycosylated Hyp units were obtained from Naziga et al.[27] Implicit solvent calculations used a generalized Born model developed by Onufriev, Bashford, and Case,[46,47] while explicit water molecules were represented by the TIP3P model.[48] Further details of each type of calculation implemented are given below.

MD Simulations in Explicit Water. The conformations of all three peptides were sampled using standard MD simulations. Initial models (adopting an ideal PPI or PPII conformation) were created with the xLEaP module of AMBER and solvated in a 48, 48, and 52 Å octahedral box of water for $(Pro)_9$, $(Hyp)_9$, and $[Hyp-(\beta\text{-Gal})]_9$, respectively. Two stages of minimization were carried out. In the first step, the solute molecule was held fixed, while the water molecules were relaxed. Next, the entire system was minimized. The resulting structures were slowly heated from 5 to 300 K over 50 ps and allowed to further equilibrate at the final temperature for another 50 ps in an NVT simulation. The equilibrated systems were then subjected to NPT production calculations of 101, 103, and 82 ns for $(Pro)_9$, $(Hyp)_9$ and $[Hyp-(\beta\text{-Gal})]_9$, respectively, in the PPII conformation. A 100 ns calculation was carried out for $(Hyp)_9$ and $[Hyp-(\beta\text{-Gal})]_9$ in the PPI conformation. A time step of 0.1 fs was used in the NVT equilibration, and 0.2 fs was used in the NPT calculations. van der Waals interactions were consistently truncated at 10 Å.

REMD Simulations in Explicit Water. REMD[49] simulations were implemented for the $(Hyp)_9$ and $[Hyp-(\beta\text{-Gal})]_9$ peptides starting from the final structures obtained from the regular MD simulations. A total of 36 replicas were implemented for $(Hyp)_9$ with the temperature ranging from 290.5 to 492.5 K, while 48 replicas and temperatures between 296.0 and 552.6 K were employed for $[Hyp-(\beta\text{-Gal})]_9$. During these simulations, the ω dihedral angle was constrained to represent the *trans* conformation (ω = 180 ± 30°) by applying a 50.0 kcal mol^{-1} rad^{-1} restraint force. This was done to comprehensively explore the PPII conformation, as well as to identify any significant deviations from the PPII structure that do not involve *trans* to *cis* isomerization. Exchanges were attempted every 125 MD steps, while all other parameters were the same as discussed for the regular NPT MD simulation. However, REMD calculations were carried out in the NVT ensemble. A 50 and 100 ns simulation per replica was implemented, which led to a total simulation time of 1.8 and 4.8 μs for $(Hyp)_9$ and $[Hyp-(\beta\text{-Gal})]_9$, respectively.

ABMD Simulations. To overcome the barriers associated with peptide *cis* to *trans* isomerization, ABMD[50,51] simulations were implemented. ABMD is effectively an umbrella sampling method that makes use of a time-dependent potential to bias the dynamics of the molecular system. This flattens the potential energy surface (PES) with respect to a selected collective variable that is related to the property under study. The ABMD implementation used in this study is based on the following equations:

$$m_i \frac{\partial^2 r_i}{\partial t^2} = F_i + \frac{\partial}{\partial r_i} U[t|\sigma(r_1, r_2, ..., r_N)]$$

$$\frac{\partial U(t|\xi)}{\partial t} = \frac{k_B T}{\tau_F} G\xi|\sigma(r_1, r_2, ..., r_N)$$

The first equation (Newton's equation of motion) defines the force acting on particle m_i at position $\mathbf{r}_i$ during time t together with a biasing potential U, which evolves according to the second equation. The biasing potential is defined in terms of a collective variable $\sigma(\mathbf{r}_1,\mathbf{r}_2,...,\mathbf{r}_N)$, which is dependent on the coordinates of the system. This potential is zero at the beginning of the simulation, but accumulates over time and, in principle, exactly negates the potential energy in terms of the defined collective variable and thereby flattens the PES. This means that $U(t|\xi) + f(\xi)$ is exactly zero, where $f(\xi)$ is the potential of mean force (PMF) (or the Landau free energy defined as $f(\xi) = -k_B T \ln p(\xi)$) and $p(\xi)$ is the probability density estimate ($p(\xi) = \langle\delta[\xi - \sigma(\mathbf{r}_1,\mathbf{r}_2,...,\mathbf{r}_N)]\rangle$). The application of ABMD requires the choice of two parameters: the flooding time, τ_F, and the kernel width, $4\Delta\xi$, which is related to the resolution of the kernel $G(\xi)$. Further details about ABMD are provided in refs 40 and 41. As in recent ABMD studies of oligoprolines,[52−54] the following collective variable was used, which is based on the cosines of the ω dihedral angle:

$$\Omega = \sum_i \cos(\omega_i)$$

Thus, Ω sums to +9 and −9 for PPI (all-*cis* or ω = 0°) and PPII (all-*trans* or ω = 180°, Figure 1) structures, respectively. In the present work, two variations of ABMD were implemented: (1) a replica exchange variant with each replica at a different temperature and biased by different potentials; and (2) a multiple walker strategy with all replicas at one temperature and biased by the same potential. Within this scheme, the following four simulation types were carried out:

a. ABMD Flooding in Implicit Water. To obtain a rough estimate of the PMF, implicit solvation was used in the first instance since it is very computationally expensive to derive the biasing potential from explicit solvent calculations. However, once a PMF is developed in implicit solvent, refinement in

dx.doi.org/10.1021/jp312487v | J. Phys. Chem. B 2013, 117, 2671−2681

Table 1. Average Number of Water Molecules That Solvate the Backbone Carbonyl Groups in the $(Pro)_9$, $(Hyp)_9$, and $[Hyp-(\beta\text{-Gal})]_9$ Peptides in the PPII Conformation According to MD Simulations in Explicit Water[a]

residue (i)	1	2	3	4	5	6	7	8	9
$(Pro)_9$	2.73	2.52	2.51	2.50	2.50	2.51	2.49	2.53	3.31
$(Hyp)_9$	2.72	2.45	2.47	2.47	2.47	2.48	2.46	2.52	3.35
$[Hyp-(\beta\text{-Gal})]_9$	1.99	1.76	1.81	1.74	1.62	1.48	2.07	2.60	3.41

[a]Solvation was determined to occur if the water molecule was within 3.4 Å of the backbone.

Table 2. Comparison of the Average Number of Water Molecules That Solvate the Backbone Carbonyl Groups in the PPII and PPI Conformations of the $(Hyp)_9$ and $[Hyp-(\beta\text{-Gal})]_9$ Peptides According to MD Simulations in Explicit Water[a]

residue (i)		1	2	3	4	5	6	7	8	9
$(Hyp)_9$	PPII	2.72	2.45	2.47	2.47	2.47	2.48	2.46	2.52	3.35
	PPI	2.62	1.99	1.67	1.46	1.44	1.46	1.45	1.42	2.04
$[Hyp-(\beta\text{-Gal})]_9$	PPII	1.99	1.76	1.81	1.74	1.62	1.48	2.07	2.60	3.41
	PPI	1.84	1.66	1.71	0.13	0.58	1.20	0.29	0.82	1.80

[a]Solvation was determined to occur if the water molecule was within 3.4 Å of the backbone.

explicit solvent becomes computationally feasible. Therefore, initially, a short 12 ns simulation was conducted for $(Pro)_9$ in implicit water at 1200 K, which employed 24 replicas, a multiple walker approach, τ_F = 25 ps and $4\Delta\xi$ = 0.2. A 1.0 fs MD time step and infinite cut-off for the nonbonded interactions were implemented. Within this period, the collective variable explored most parts of the PES (i.e., Ω evolved from −9 to +9 several times). Using this estimate as input, more refined flooding calculations were performed with $4\Delta\xi$ reduced to 0.1 and τ_F increased in stages from 25 to 200 ps. At this stage, 24 replicas were implemented, each with a different biasing potential and temperatures ranging from 300 to 1200 K, where the wide temperature range (300−1200 K) will aid transition between the PPII and PPI structures. A total of 328 ns per replica simulation was used to refine the PMF for $(Pro)_9$. Using this refined potential, τ_F = 100 and 200 ps, a PMF for $(Hyp)_9$ was obtained from an additional 200 ns per replica simulation. Similarly, using PMFs from $(Hyp)_9$ and a 150 ns per replica simulation, the PMF for $[Hyp-(\beta\text{-Gal})]_9$ was obtained.

b. Umbrella Sampling Corrections to the PMF. The PMFs obtained from the flooding stage described above were used in umbrella sampling calculations. This approach is based on the principle that if the PMF is very close to the exact value, then a flat histogram will be obtained in the space of the collective variable or, in other words, all values will be equally accessible. However, if there is a small difference (a few k_BT) between the calculated PMF and the true value, then the histogram obtained from umbrella sampling can serve as a correction. For each peptide under study, umbrella sampling simulations were conducted for at least 250 ns per replica and used to correct the PMFs. The same number of replicas and temperature range were employed as discussed for the flooding calculations.

c. HT-REMD Calculations. To obtain equilibrium data from the ABMD calculations, an HT-REMD scheme was implemented using PMFs from the flooding stage. In these calculations, a total of 28 replicas (rather than the 24) were used. At 300 K, one of the four additional replicas is completely unbiased, while the other three additional replicas are biased based on the PMF of the 300 K replica and scaled by a range of factors (0.49, 0.76 or 0.90) that have been previously used and shown to work well for these types of systems.[29] This procedure enhances the exchange to the unbiased replica. All other simulation parameters were the same as for the flooding simulations. These calculations were run for at least 250 ns per replica for each peptide.

d. PMF Refinement in Explicit Water. For the $(Hyp)_9$ and $[Hyp-(\beta\text{-Gal})]_9$ peptides, calculations were conducted in explicit solvent to determine the discrete effects of water on the calculated PMFs. As done previously, PMFs obtained from the implicit solvent flooding stage were used as the starting point. Due to the large number of replicas required to cover the (300−1200 K) temperature range in an explicit solvent calculation, all 24 replicas were simulated at 300 K using a multiple walker approach. Initial structures of the solute in TIP3P water were taken from the explicit solvent REMD calculations. All other simulation parameters were the same as for REMD and ABMD, with the exception that the nonbonded cut-offs and time step were reduced to 8.0 Å and 1.0 fs, respectively.

RESULTS

Intermolecular/Intramolecular Interactions and Structural Information from MD Simulations in Explicit Water. Initially, equilibrium MD simulations were performed on $(Pro)_9$, $(Hyp)_9$, and $[Hyp-(\beta\text{-Gal})]_9$ (Figure 3) in explicit water. In the analysis of these simulations, a particular focus is placed on hydration and intramolecular hydrogen bonding. This choice was made since it is well-known that interactions between solvent (water) molecules and the peptide backbone are important for maintaining the PPII conformation in polyproline helices, which does not contain backbone-to-backbone intramolecular interactions.[55,56] Additionally, the preferential stability of PPII relative to PPI is solvent dependent for unsubstituted polyproline, with PPII being the most stable structure in polar solvents and PPI favored in aliphatic alcohols.[57−59] Nevertheless, glycosylation may change solvent accessibility and/or introduce new intramolecular hydrogen bonding to the peptide backbone.

To gain insight into backbone hydration, the first water shell of the peptides was analyzed to determine the number of solvent molecules potentially able to form water−backbone interactions. Using a cut-off of 3.4 Å, which coincides with the first minimum in the water−backbone C═O radial distribution function, the number of water molecules in the vicinity of the backbone carbonyl groups was counted. The resulting averages over the duration of the MD simulations for the peptides in the PPII conformation are presented in Table 1 for each residue

dx.doi.org/10.1021/jp312487v | J. Phys. Chem. B 2013, 117, 2671−2681

(1−9) in the peptide with the capping groups ignored. The number of water molecules solvating the carbonyl backbone of $(Pro)_9$ and $(Hyp)_9$ are nearly identical, which indicates that the backbone solvation is not affected by hydroxylation. However, there is an overall slight (0.5−1) decrease in solvation of the backbone upon complete glycosylation of $(Hyp)_9$ since the bulky sugar groups shield the backbone from water. These results are consistent with an observed decrease in the CD maxima for the glycosylated peptide compared to $(Hyp)_9$,[31] which was in part attributed to a change in the solvation environment of the backbone[31] and is now confirmed for the first time by our MD results.

We also examined the backbone solvation of the PPI conformation in both the hydroxylated and glycosylated compounds to determine whether differences in the experimentally observed thermal stability[31] can be attributed to variations in the solvation of PPI and PPII (Table 2). We find that, on average, fewer water molecules interact with the backbone in the PPI conformation of both peptides. This is in line with experimental[57,59] and computational studies,[52] which show that the PPI conformation is not favored in water due to loss of backbone−water hydrogen-bonding interactions. This finding also correlates with the more compact structure of the PP1 conformation (Figure 2).

As expected, no intramolecular interactions were found in the $(Pro)_9$ and $(Hyp)_9$ peptides in the PPII conformation. However, several peptide−sugar and sugar−sugar interactions are present in $[Hyp-(\beta\text{-Gal})]_9$ (Table S1, Supporting Information). Overall, these contacts occur for a small portion of the MD calculation, with a maximum occupancy of approximately 13%, since there is competition between the backbone carbonyls and water for interactions with the sugar hydroxyl groups (>84%, Table S2). The sugar−backbone hydrogen-bonding interactions that occur for at least 5% of the total simulation time include interactions between the O6′-hydroxyl hydrogen at position i and the carbonyl oxygen (C═O) in the peptide backbone at positions $i-2$ and $i-3$ (Figures 4 and S2A,B). Additionally, hydrogen bonding occurs between the O2′ hydrogen of residue i and O6′ of residue $i+1$ (Figure S2C). Despite the large number of such interactions, their low occupancies indicate that intramolecular hydrogen bonding cannot explain the increased thermal stability of $[Hyp-(\beta\text{-Gal})]_9$ relative to $(Pro)_9$ and $(Hyp)_9$.

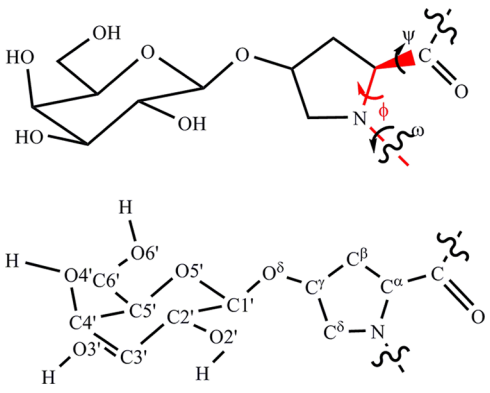

Figure 4. Definitions of various dihedral angles (top) and atomic numbering (bottom) in the galactosylated hydroxyproline residue.

Compared with the PPII conformation, intramolecular hydrogen bonds are observed in the PPI conformation with a higher frequency (Table S3). Indeed, several peptide−sugar and sugar−sugar interactions exist, with six of these having occupancies over 50%. The peptide−sugar interactions primarily occur between the O6′-hydroxyl hydrogen at position i and the carbonyl oxygen (C═O) in the peptide backbone at position $i-1$ (Figure S3A). Sugar−sugar interactions mainly take place between the O2′ (O4′) hydrogen of residue i and O6′ of residue $i+3$ ($i+3$) (Figure S3B,C). Therefore, while solvent−backbone hydrogen bonding is greatly reduced in the PPI conformation of the $[Hyp-(\beta\text{-Gal})]_9$ peptide, strong intramolecular interactions appear.

The backbone (ϕ,ψ) dihedral angles for the calculations carried out in the PPII conformation adopt average values of (−63°, 155°), (−61°, 153°) and (−65°, 160°) for $(Pro)_9$, $(Hyp)_9$, and $[Hyp-(\beta\text{-Gal})]_9$, respectively. Furthermore, all ω dihedral angles in the three peptides remain close to 180°. This indicates that all three peptides remain in the PPII conformation for the duration of the calculation as expected based on previous literature.[39,41,52] While the length of these simulations is sufficient to obtain equilibrium information about the PPII conformation, it may not be sufficient to overcome barriers to other possible low energy states on the PES. For instance, other peptides that significantly populate the PPII conformation can also adopt β-strand conformations.[60−67] In addition, it would be interesting to determine whether structures that significantly deviate from the PPII conformation can be adopted without invoking *trans* to *cis* isomerization. This will clarify proposals in the literature that isomerization is the main source of conformational heterogeneity in oligoproline peptides.[28,30,68] To address these questions, REMD simulations on the $(Hyp)_9$ and $[Hyp-(\beta\text{-Gal})]_9$ peptides will be discussed in the next section. The $(Pro)_9$ peptide was not considered with REMD since the data presented in this section suggests that this peptide and $(Hyp)_9$ have similar solvation properties. Additionally, the most likely explanation for the observed increased PPII stability of $(Hyp)_9$ relative to $(Pro)_9$ is increased *trans* stabilization due to a stereoelectronic effect.[17,18,20,21]

Structural Information from REMD Simulations in Explicit Water. To comprehensively explore the PPII conformation, as well as identify significant deviations from the PPII structure that do not involve a *trans* to *cis* isomerization, a restraint force was applied in the REMD simulations in explicit water to constrain the ω dihedral angle to represent the *trans* conformation.

Table 3 displays the average number of water molecules within 3.4 Å of the peptide backbone carbonyls in the $(Hyp)_9$ and $[Hyp-(\beta\text{-Gal})]_9$ peptides at room temperature and the highest temperature simulated. Solvation of the backbone carbonyl groups does not significantly deviate with temperature for either peptide. However, the intramolecular hydrogen-bond occupancy deceases with increased temperature for the $[Hyp-(\beta\text{-Gal})]_9$ peptide (Table S1). Indeed, at the highest temperature considered (552.6 K), all but one peptide−sugar and sugar−sugar intramolecular hydrogen bond is lost in the glycosylated peptide (depicted in Figure S2B).

The PPII content versus temperature is displayed in Figure 5, where a given residue was considered to adopt a PPII conformation if $(-110° < \phi < -20°)$, $(50° < \psi < 180°)$, or $(-120° < \psi < -180°)$, and the ω dihedral angle adopts a *trans* configuration. The data indicates that, even at very high temperatures, the ϕ and ψ dihedral angles remain in the PPII region of the Ramachandran plot in both peptides when ω is constrained to the *trans* conformation. Analysis of the data

dx.doi.org/10.1021/jp312487v | J. Phys. Chem. B 2013, 117, 2671−2681

Table 3. Comparison of the Average Number of Water Molecules That Solvate the Backbone Carbonyl Groups of the $(Hyp)_9$ and $[Hyp-(\beta\text{-Gal})]_9$ Peptides at Different Temperatures According to REMD Simulations in the PPII Conformation[a]

residue (i)		1	2	3	4	5	6	7	8	9
$(Hyp)_9$	299.4 K	2.72	2.51	2.45	2.48	2.49	2.49	2.47	2.53	3.35
	492.5 K	2.79	2.57	2.55	2.58	2.55	2.56	2.54	2.67	3.72
$[Hyp-(\beta\text{-Gal})]_9$	300.0 K	1.98	1.68	1.70	1.69	1.64	1.54	2.06	2.58	3.40
	552.6 K	2.29	1.99	1.97	2.00	1.95	1.99	2.12	2.72	3.81

[a]Solvation was determined to occur if the water molecule was within 3.4 Å of the backbone.

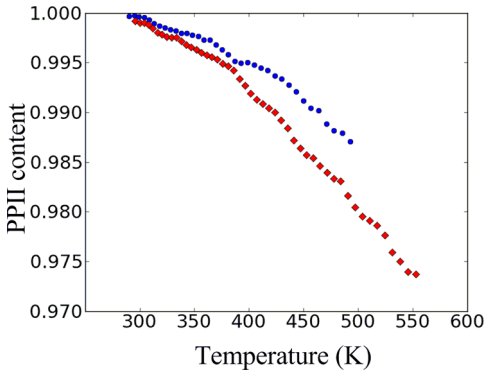

Figure 5. Change in PPII content as a function of temperature according to REMD simulations of the Ac–$(Hyp)_9$–NH_2 (blue, circle) and Ac–$[Hyp-(\beta\text{-D-Gal})]_9$–$NH_2$ (red, diamond) peptides in explicit water.

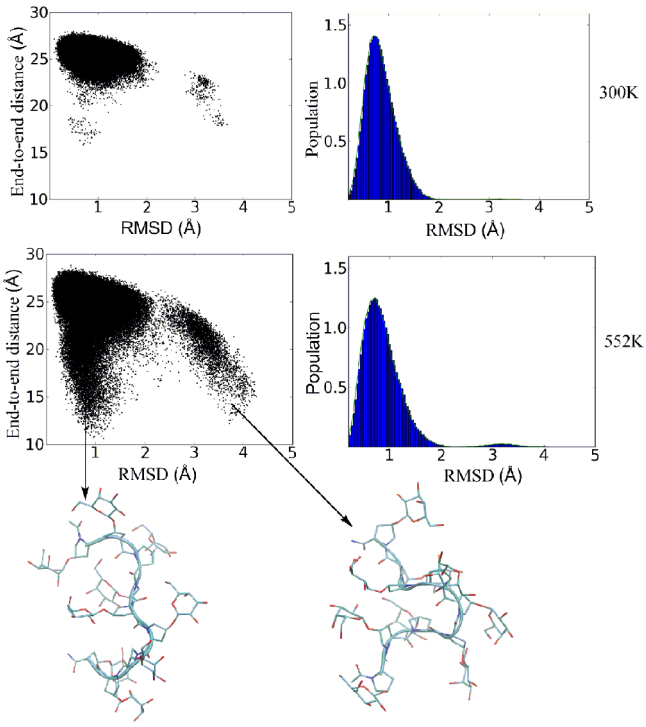

Figure 6. End-to-end distance (N in P_1 to CA in P_9) versus RMSD from an ideal PPII structure (left) and RMSD histograms (right) obtained from explicit solvent REMD calculations on the Ac–$[Hyp-(\beta\text{-D-Gal})]_9$–$NH_2$ peptide at 300 K (top) and 552 K (bottom). Representative structures are shown for the conformations with the large deviations from an ideal PPII helix.

reveals a mostly PPII family of structures with a root-mean-square deviation (RMSD) of ≈1–2 Å from an idealized PPII and end-to-end distances of approximately 22–28 Å (Figure 6). However, there are a few excursions from an idealized PPII structure to more globular-like structures (RMSD ≈ 3–4 Å). These globular structures arise in both peptides when $\psi \approx -50°$ in the residues in the center region of the peptide (i = 4–5), which defines the α_R-configuration. The number of such transitions increases with temperature (Figure 6), but corresponds to a very small portion of the total trajectory.

The above homogeneous results indicate that *cis–trans* isomerization is likely the most important factor in the observed conformational heterogeneity of oligoprolines and derivatives. Specifically, when the PPII conformation melts, *cis* conformations must be adopted. Additionally, there is no evidence of β-sheet or random coil structures, even at high temperatures. To determine whether the conformational ensemble changes when the restraint on ω is removed and gain free estimates for conversion between the PPI and PPII conformations, ABMD calculations were conducted as described in the following sections.

ABMD Simulations in Implicit Water. ABMD simulations were initially carried out in implicit water to investigate the influence of *cis–trans* isomerization on the structural ensemble of all peptides (Figure 3) since this transition does not occur on feasible time scales during regular dynamics. As mentioned in the Methods, implicit solvation was used in the first instance since it is very computationally expensive to derive the biasing potential from explicit solvent calculations. Furthermore, a wide temperature range (300–1200 K) was implemented in the implicit solvent calculations to aid transition between the PPII and PPI structures. This combination of temperature and umbrella (ABMD) sampling has been previously shown to adequately characterize the conformational dynamics of polyproline peptides.[52,54] Initial calculations were performed on $(Pro)_9$ for comparison to previous studies, as well as to obtain a PMF that can be extended to the $(Hyp)_9$ and $[Hyp-(\beta\text{-Gal})]_9$ models.

From the PMFs (Figure 7), the free energy for transitioning from PPII to PPI (ΔF(PPII–PPI)) is estimated to be −4.9 kcal mol^{-1}, −9 kcal mol^{-1}, and −9 kcal mol^{-1} for $(Pro)_9$, $(Hyp)_9$, and $[Hyp-(\beta\text{-Gal})]_9$, respectively. The more negative ΔF(PPII–PPI) for $(Hyp)_9$ and $[Hyp-(\beta\text{-Gal})]_9$ relative to $(Pro)_9$ is expected since these PTMs have been shown to stabilize the *trans* conformation.[23] The resulting PMFs were subsequently used in HT-REMD simulations, which included an unbiased replica to obtain equilibrium data. A residue-based analysis was subsequently performed to determine the percentage of conformations that adopt the PPII structure (P(PPII)), *trans* ω dihedral angle (P(T)), as well as lie in the F region of the Ramachandran plot (P(F)), which encompasses both PPI and PPII structures (Table 4).

The unbiased HT-REMD data indicates a high PPII content in the $(Pro)_9$ peptide, with P(PPII) ranging between 56 and 86% and on average being 65%. However, P(T) is on average 69%, which implies there is a significant amount of the *cis*

dx.doi.org/10.1021/jp312487v | J. Phys. Chem. B 2013, 117, 2671–2681

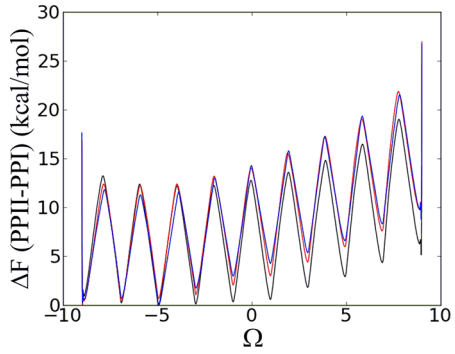

Figure 7. PMF for conversion from PPII (Ω = −9.0) to PPI (Ω = +9.0) for the Ac−$(Pro)_9$−NH_2 (black), Ac−$(Hyp)_9$−NH_2 (red), and Ac−[Hyp−(β-D-Gal)]$_9$−NH_2 (blue) peptides obtained from implicit solvent ABMD simulations.

conformation about the ω dihedral (31%). Furthermore, there is a decrease in the percentage occupation of the *trans* isomer toward the middle of the peptide. Specifically, the occupation decreases from 74% for the first Pro residue (Ac−P_1) to 55% for the fifth residue (P_4−P_5), and increases to 90% for the final residue (P_8−P_9). The *P*(F) region is occupied for approximately 100% of the simulation for all residues in the strand except for the last prolyl amide bond. Similar results have been obtained in other computational studies of oligoprolines,[28,29] which verifies our approach.

There is an increase in the number of *trans* conformers in both modified peptides relative to $(Pro)_9$, which is expected since the PTMs have been shown to enhance the *trans* conformation.[23,69] Indeed, the *trans* amide isomer exists for an average of 86% and 87% of the simulation time in $(Hyp)_9$ and [Hyp−(β-Gal)]$_9$, respectively. Furthermore, *P*(PPII) is on average 83% for both peptides. Similar to $(Pro)_9$, *P*(F) is nearly 100% in all but the last residue in both modified peptides.

The probability that a particular conformational sequence is adopted was obtained from a sequence-based analysis of the equilibrium data that determines whether each peptide residue adopts the *cis* or *trans* conformation. The results of this analysis are shown in Table 5 for the seven most likely sequences. In the $(Pro)_9$ peptide, the all-*trans* sequence is the most probable conformation. However, this sequence has a low probability (3.3%) and a strand with *cis* interruption in the middle has a very close probability. This implies that the $(Pro)_9$ oligomer likely adopts an ensemble of structures with consecutive *trans* residues interspaced by *cis* residues at 300 K. This result is in line with several recent experimental and computational findings.[28−30] More importantly, our calculations show a significant increase in the all-*trans* sequence in both the $(Hyp)_9$ and [Hyp−(β-Gal)]$_9$ peptides (26.5 and 27.8%, respectively) relative to $(Pro)_9$ (3.3%). This finding correlates with the experimentally observed extra stabilization of the *trans* isomer due to these modifications.[23]

Using the HT-REMD data, Δ*F*(PPII−PPI) is estimated to be −4.9, −10.1, and −11.0 kcal mol^{-1} for $(Pro)_9$, $(Hyp)_9$, and [Hyp−(β-Gal)]$_9$, respectively. These values are very similar to those obtained from the PMFs, which suggests that both sets of calculations are well converged. However, experimental T_m values show that the glycosylated peptide (T_m = 70 °C) is more stable than the hydroxylated peptide (T_m = 38 °C), which should translate to a significantly more negative calculated Δ*F* for the glycosylated peptide relative to $(Hyp)_9$. It is anticipated that the absence of explicit water molecules in the ABMD calculations could be responsible for this discrepancy. To test this hypothesis, explicit solvent refinement of the implicit solvent PMFs was performed for the $(Hyp)_9$ and [Hyp−(β-Gal)]$_9$ peptides as discussed below. $(Pro)_9$ is not considered in this analysis since the corresponding PMF is already much smaller than that of $(Hyp)_9$, which correlates well with experiment.[31]

ABMD Simulations in Explicit Water. Multiple walker ABMD simulations at 300 K were used to refine the PMFs obtained in implicit solvent. Comparison of the results obtained in explicit solvent for $(Hyp)_9$ and [Hyp−(β-Gal)]$_9$ (Figure 8) suggests that explicit water molecules have a profound effect on the PMFs. In $(Hyp)_9$, Δ*F*(PPII−PPI) is approximately −20 kcal mol^{-1} in explicit solvent compared to −9 kcal/mol in implicit solvent (Figures 7 and 8A). An even larger effect occurs for the [Hyp−(β-Gal)]$_9$ peptide, where the free energy difference decreases to approximately −46 kcal mol^{-1} from −9 kcal mol^{-1} (Figures 7 and 8B). Therefore, the state-of-the-art ABMD calculations in explicit water suggest that the PPII structures are more strongly preferred relative to PPI by 26 kcal mol^{-1} in [Hyp−(β-Gal)]$_9$ compared to $(Hyp)_9$. This finding is consistent with the experimentally observed T_m values for the two peptides, suggesting that discrete sugar−solvent and peptide−solvent interactions are likely responsible for the increased thermal stability of the glycosylated peptide. A similar

Table 4. PPII and *trans* Content of Each Residue in All Model Compounds Obtained from Unbiased HT-REMD Simulations in Implicit Water

	$(Pro)_9$			$(Hyp)_9$			[Hyp−(β−Gal)]$_9$		
bond	*P*(PPII)[a]	*P*(T)[b]	*P*(F)[c]	*P*(PPII)[a]	*P*(T)[b]	*P*(F)[c]	*P*(PPII)[a]	*P*(T)[b]	*P*(F)[c]
Ac−P_1	74	74	100	77	77	99	72	74	100
P_1−P_2	75	76	100	89	89	100	90	92	98
P_2−P_3	64	65	100	87	88	100	96	96	100
P_3−P_4	61	61	100	85	84	100	84	81	100
P_4−P_5	56	55	100	87	87	100	80	81	100
P_5−P_6	56	58	100	82	83	98	88	89	99
P_6−P_7	61	62	100	87	87	100	82	85	99
P_7−P_8	86	87	100	89	91	99	90	94	97
P_8−P_9	56	90	67	67	91	76	64	90	75
Average	65	69		83	86		83	87	

[a]*P*(PII) refers to the percentage of time that a residue adopts the PPII conformation. [b]*P*(T) refers to the percentage of time that a residue adopts the *trans* conformation. [c]*P*(F) denotes the percentage of time spent in the F region (PPI and PPII) of the Ramachandran plot.

dx.doi.org/10.1021/jp312487v | J. Phys. Chem. B 2013, 117, 2671−2681

Table 5. The Seven Most Probable Conformers of the $(Pro)_9$, $(Hyp)_9$, and $[Hyp-(\beta\text{-Gal})]_9$ Peptides in Terms of the *cis* (C) or *trans* (T) Conformation about the ω Dihedral Angle for Each Residue According to Unbiased HT-REMD Simulations in Implicit Water

$(Pro)_9$		$(Hyp)_9$		$[Hyp-(\beta\text{-Gal})]_9$	
sequence	prob. (%)	sequence	prob. (%)	sequence	prob. (%)
TTTTTTTTT	3.3	TTTTTTTTT	26.5	TTTTTTTTT	27.8
TTTTCTTTT	3.0	CTTTTTTTT	7.9	CTTTTTTTT	9.7
TTTTTCTTT	2.4	TTTTTCTTT	5.3	TTTCTTTTT	6.4
TTTTCCTTT	2.2	TTTCTTTTT	4.9	TTTTCTTTT	6.2
TTTCTTTTT	2.1	TTTTCTTTT	3.9	TTTTTTCTT	5.0
TTTTTTCTT	1.9	TTTTTTCTT	3.9	TTTTTCTTT	3.3
TTTCCTTTT	1.9	TTCTTTTTT	3.8	TTTTTTTTC	3.2

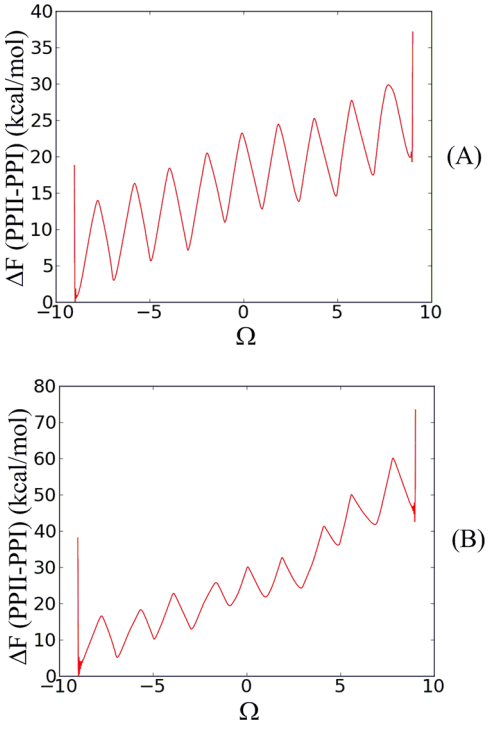

Figure 8. Potential of mean force (ΔF(PPII−PPI)) for conversion from PPII (Ω = −9.0) to PPI (Ω = +9.0) for the (A) Ac−$(Hyp)_9$−NH_2 and (B) Ac−$[Hyp-(\beta\text{-D-Gal})]_9$−$NH_2$ peptides obtained from explicit solvent ABMD simulations.

effect of sugar−explicit solvent interactions has been previously reported in the literature for an *N*-glycosylated protein.[33]

DISCUSSION

Experimental results have shown that Pro modifications can increase the structural integrity of oligoproline peptides.[20,31] In particular, contiguous galactosylation of a nonaproline oligomer, which is a viable model of the HRGPs found in plant cell walls, leads to a higher melting temperature compared to the corresponding hydroxylated model.[31] The stabilizing effects due to contiguous hydroxylation can be understood in terms of stereoelectronic ($n \rightarrow \pi^*$) effects that favor the *trans* conformation. However, the reason for the increased stability due to glycosylation cannot be fully attributed to such effects since glycosylation and hydroxylation yield similar *trans* preferences in monomeric units.[24] To explain this experimental observation, the present work outlines detailed conformational sampling of three oligoproline peptides: $(Pro)_9$, $(Hyp)_9$, and $[Hyp-(\beta\text{-Gal})]_9$.

A covalently linked sugar can stabilize a particular peptide conformation via different modes of action.[33−35] First, the glycan could form strong intramolecular hydrogen bonds to the peptide backbone and/or other glycans. Indeed, this has been proposed in the literature to explain why certain oligomers containing other amino acid residues, such as glutamines (Gln), have a high tendency to form PPII helices.[70] In this case, calculations show that the Gln side chain forms a hydrogen bond to the preceding main chain carbonyl group, which maintains the ψ dihedral of the Gln residue, and the ϕ and ψ angles of the preceding residue in the PPII conformation. In the case of β-D-galactose addition, our data shows that there are indeed similar intramolecular hydrogen-bonding interactions between neighboring sugars and between the sugars and the peptide backbone. Specifically, interactions exist between the O6′-hydroxyl hydrogen (Figure 4) at position *i* and the carbonyl oxygen (C═O) in the peptide backbone at positions *i*−2 and *i*−3. Additionally, hydrogen bonding occurs between the O2′ hydrogen of residue *i* and O6′ of residue *i*+1. However, in the presence of explicit solvent molecules, there is a competition between intramolecular interactions and intermolecular interactions with solvent. Indeed, there is a maximum occupancy of only 13% for the sugar−backbone and sugar−sugar interactions in an 80 ns MD simulation. Thus, while the observed intramolecular hydrogen bonding may contribute to the stability of the PPII conformation, it will not lead to the observed 37 °C difference in the melting temperature of $(Hyp)_9$ and $[Hyp-(\beta\text{-Gal})]_9$. This contradicts the previous proposal (based on preliminary molecular mechanics minimizations) that intramolecular hydrogen bonding is responsible for differences in the $(Hyp)_9$ and $[Hyp-(\beta\text{-Gal})]_9$ melting temperatures.[31]

The covalently linked sugars can also lead to a favored PPII conformation through a steric mechanism. Specifically, more energy could be required to transition from a PPII to PPI conformation because of steric clashes during the *cis* to *trans* isomerization. While this may be true for biological HRGP with complex polysaccharides attached,[71] our calculations do not support this proposal for the increased PPII stability in $[Hyp-(\beta\text{-Gal})]_9$. Indeed, PMFs obtained from implicit solvent ABMD calculations are almost identical for $(Hyp)_9$ and $[Hyp-(\beta\text{-Gal})]_9$ (Figure 7), which leads to very close estimated free energy differences between PPI and PPII. Likewise, the HT-REMD free energy estimates, as well as the estimated proportion of the all-*trans* PPII sequence (Table 5), are very close for both oligopeptides.

Combined, the observations outlined in the previous two paragraphs led us to refine the PMFs in explicit (water) solvent, and the subsequent analysis reveals the likely reason for the

dx.doi.org/10.1021/jp312487v | J. Phys. Chem. B 2013, 117, 2671−2681

observed increased stability of the glycosylated peptide. Specifically, the PPII conformation of Hyp and [Hyp−(β=Gal)]$_9$ (Figure 8) are more stabilized relative to PPI in explicit solvent compared to the implicit solvent. However, this effect is greater for [Hyp−(β-Gal)]$_9$. Therefore, the ΔF(PPII−PPI) for [Hyp−(β-Gal)]$_9$ in explicit water is approximately 26 kcal mol^{-1} lower than predicted for the hydroxylated peptide, which agrees with experiment.[31] Since implicit solvent does not allow direct hydrogen bonding between the solvent and the backbone or sugar, the only available explanation for the difference in ΔF(PPII−PPI) for (Hyp)$_9$ versus [Hyp−(β-Gal)]$_9$ is that the sugars interact with the water molecules in some fashion that makes the PPII form much more stable. This interaction is likely hydrogen bonding between the sugar hydroxyl groups and water molecules. Our equilibrium MD calculations in explicit solvent show that these hydrogen bonds are present most of the time and are only briefly interrupted by intramolecular hydrogen bonding to other sugars or the peptide backbone (Table S2). Conversion of a peptide bond from the *trans* to *cis* configuration would require a disruption of this hydrogen-bonding network and displacement of water molecules around the peptide. Interestingly, several solvent−hydroxyl hydrogen bonds are also observed in the hydroxylated derivatives, which have been highlighted previously in the literature[18] and may work with stereoelectronic effects to contribute to the greater PPII stability of these oligomers compared to (unsubstituted) oligoprolines.

In summary, our extensive MD calculations suggest that interactions between the sugar moieties covalently attached to an oligoproline peptide and the surrounding water molecules lead to an increased stability of the PPII conformation. Additionally, this explains the recent experimental findings that contiguously galactosylated peptides exhibit higher melting temperatures compared to the corresponding unglycosylated or contiguously hydroxylated peptides.[31] Our results highlight a potential mode of action for complex glycans. This includes, for example, those in the HRGPs of plant cell walls, which are extensively glycosylated with complex carbohydrates that have been proposed to be responsible for their structural integrity.[15] Further work considering noncontiguous glycosylation, as well as substitution of proline with alanine or serine, is currently in progress to provide more structural insight into other biologically relevant proline containing sequences.

■ ASSOCIATED CONTENT

Supporting Information

Tables containing details and Figures of the intermolecular and intramolecular hydrogen-bonding interactions at different temperatures observed in the Ac-[Hyp-(β-D-galactose)]$_9$-NH$_2$ peptide. This material is available free of charge via the Internet at http://pubs.acs.org.

■ AUTHOR INFORMATION

Notes

The authors declare no competing financial interest.

■ ACKNOWLEDGMENTS

This research was supported by the Natural Sciences and Engineering Research Council (NSERC) of Canada and the Canada Foundation for Innovation (CFI), as well as the Canada Research Chair (CRC) program for S.D.W. and the University of Lethbridge for E.B.N. Calculations were conducted using resources available through the Western Canada Grid (WestGrid and Compute/Cacul Canada) and the Upscale and Robust Abacus for Chemistry In Lethbridge (URACIL). We would also like to thank C. Sagui, V. Babin and M. Moradi for assistance with the ABMD calculations.

■ REFERENCES

(1) Adzhubei, A. A.; Sternberg, M. J. E. Left-handed polyproline-II helices commonly occur in globular-proteins. *J. Mol. Biol.* **1993**, *229*, 472−493.
(2) Shi, Z. S.; Chen, K.; Liu, Z. G.; Kallenbach, N. R. Conformation of the backbone in unfolded proteins. *Chem. Rev.* **2006**, *106*, 1877−1897.
(3) Kay, B. K.; Williamson, M. P.; Sudol, P. The importance of being proline: The interaction of proline-rich motifs in signaling proteins with their cognate domains. *FASEB J.* **2000**, *14*, 231−241.
(4) Mayer, B. J. SH3 domains: Complexity in moderation. *J. Cell Sci.* **2001**, *114*, 1253−1263.
(5) Pawson, T. Protein modules and signaling networks. *Nature* **1995**, *373*, 573−580.
(6) Ramachandran, G. N.; Kartha, G. Structure of collagen. *Nature* **1955**, *176*, 593−595.
(7) Kieliszewski, M. J.; Lamport, D. T. A.; Tan, L.; Cannon, M. C. Hydroxyproline-rich glycoproteins: Form and function. *Annu. Plant Rev.* **2011**, *41*, 321−342.
(8) Cannon, M. C.; Terneus, K.; Hall, Q.; Tan, L.; Wang, Y. M.; Wegenhart, B. L.; Chen, L. W.; Lamport, D. T. A.; Chen, Y. N.; Kieliszewski, M. J. Self-assembly of the plant cell wall requires an extensin scaffold. *Proc. Natl. Acad. Sci. U.S.A.* **2008**, *105*, 2226−2231.
(9) Velasquez, S. M.; Ricardi, M. M.; Dorosz, J. G.; Fernandez, P. V.; Nadra, A. D.; Pol-Fachin, L.; Egelund, J.; Gille, S.; Harholt, J.; Ciancia, M.; Verli, H.; Pauly, M.; Bacic, A.; Olsen, C. E.; Ulvskov, P.; Petersen, B. L.; Somerville, C.; Iusem, N. D.; Estevez, J. M. *O*-Glycosylated cell wall proteins are essential in root hair growth. *Science* **2011**, *332*, 1401−1403.
(10) Lamport, D. T. A. Hydroxyproline *O*-glycosidic linkage of plant cell wall glycoprotein extensin. *Nature* **1967**, *216*, 1322.
(11) Fisher, J. F.; Harrison, A. W.; Bundy, G. L.; Wilkinson, K. F.; Rush, B. D.; Ruwart, M. J. Peptide to glycopeptide: Glycosylated oligopeptide renin inhibitors with attenuated in vivo clearance properties. *J. Med. Chem.* **1991**, *34*, 3140−3143.
(12) Mehta, S.; Meldal, M.; Duus, J. O.; Bock, K. Evaluation of the effect of glycosylation on the enzymic hydrolysis of peptides. *J. Chem. Soc., Perkin Trans. 1* **1999**, 1445−1452.
(13) Imperiali, B. Protein glycosylation: The clash of the titans. *Acc. Chem. Res.* **1997**, *30*, 452−459.
(14) Bilsky, E. J.; Egleton, R. D.; Mitchell, S. A.; Palian, M. M.; Davis, P.; Huber, J. D.; Jones, H.; Yamamura, H. I.; Janders, J.; Davis, T. P.; Porreca, F.; Hruby, V. J.; Polt, R. Enkephalin glycopeptide analogues produce analgesia with reduced dependence liability. *J. Med. Chem.* **2000**, *43*, 2586−2590.
(15) Ferris, P. J.; Woessner, J. P.; Waffenschmidt, S.; Kilz, S.; Drees, J.; Goodenough, U. W. Glycosylated polyproline II rods with kinks as a structural motif in plant hydroxyproline-rich glycoproteins. *Biochemistry* **2001**, *40*, 2978−2987.
(16) Shoulders, M. D.; Kotch, F. W.; Choudhary, A.; Guzei, I. A.; Raines, R. T. The Aberrance of the 4S diastereomer of 4-hydroxyproline. *J. Am. Soc. Chem.* **2010**, *132*, 10857−10865.
(17) Bretscher, L. E.; Jenkins, C. L.; Taylor, K. M.; DeRider, M. L.; Raines, R. T. Conformational stability of collagen relies on a stereoelectronic effect. *J. Am. Soc. Chem.* **2001**, *123*, 777−778.
(18) Horng, J. C.; Raines, R. T. Stereoelectronic effects on polyproline conformation. *Protein Sci.* **2006**, *15*, 74−83.
(19) DeRider, M. L.; Wilkens, S. J.; Waddell, M. J.; Bretscher, L. E.; Weinhold, F.; Raines, R. T.; Markley, J. L. Collagen stability: Insights from NMR spectroscopic and hybrid density functional computational investigations of the effect of electronegative substituents on prolyl ring conformations. *J. Am. Soc. Chem.* **2002**, *124*, 2497−2505.

(20) Kuemin, M.; Nagel, Y. A.; Schweizer, S.; Monnard, F. W.; Ochsenfeld, C.; Wennemers, H. Tuning the cis/trans conformer ratio of Xaa-Pro amide bonds by intramolecular hydrogen bonds: The effect on PPII helix stability. *Angew. Chem., Int. Ed.* **2010**, *49*, 6324−6327.
(21) Sonntag, L.-S.; Schweizer, S.; Ochsenfeld, C.; Wennemers, H. The "azido gauche effect" − Implications for the conformation of azidoprolines. *J. Am. Soc. Chem.* **2006**, *128*, 14697−14703.
(22) Kuemin, M.; Sonntag, L.-S.; Wennemers, H. Azidoproline containing helices: Stabilization of the polyproline II structure by a functionalizable group. *J. Am. Soc. Chem.* **2007**, *129*, 466−467.
(23) Owens, N. W.; Braun, C.; O'Neil, J. D.; Marat, K.; Schweizer, F. Effects of glycosylation of (2S,4R)-4-hydroxyproline on the conformation, kinetics, and thermodynamics of prolyl amide isomerization. *J. Am. Soc. Chem.* **2007**, *129*, 11670−11671.
(24) Owens, N. W.; Lee, A.; Marat, K.; Schweizer, F. The implications of (2S,4S)-hydroxyproline 4-*O*-glycosylation for prolyl amide isomerization. *Chem.—Eur. J.* **2009**, *15*, 10649−10657.
(25) Zhang, K.; Teklebrhan, R. B.; Schreckenbach, G.; Wetmore, S.; Schweizer, F. Intramolecular hydrogen bond-controlled prolyl amide isomerization in glucosyl 3′(*S*)-hydroxy-5′-hydroxymethylproline hybrids: Influence of a C-5′-hydroxymethyl substituent on the thermodynamics and kinetics of prolyl amide cis/trans isomerization. *J. Org. Chem.* **2009**, *74*, 3735−3743.
(26) Teklebrhan, R. B.; Zhang, K. D.; Schreckenbach, G.; Schweizer, F.; Wetmore, S. D. Intramolecular hydrogen bond-controlled prolyl amide isomerization in glucosyl 3(*S*)-hydroxy-5-hydroxymethylproline hybrids: A computational study. *J. Phys. Chem. B* **2010**, *114*, 11594−11602.
(27) Naziga, E. B.; Schweizer, F.; Wetmore, S. D. Conformational study of the hydroxyproline-O-glycosidic linkage: Sugar-peptide orientation and prolyl amide lsomerization in (*α*/*β*)-galactosylated 4(*R*/*S*)-hydroxyproline. *J. Phys. Chem. B* **2012**, *116*, 860−871.
(28) Vila, J. A.; Baldoni, H. A.; Ripoll, D. R.; Ghosh, A.; Scheraga, H. A. Polyproline II helix conformation in a proline-rich environment: A theoretical study. *Biophys. J.* **2004**, *86*, 731−742.
(29) Moradi, M.; Babin, V.; Roland, C.; Sagui, C. A classical molecular dynamics investigation of the free energy and structure of short polyproline conformers. *J. Chem. Phys.* **2010**, *133*, 125104−125118.
(30) Doose, S.; Neuweiler, H.; Barsch, H.; Sauer, M. Probing polyproline structure and dynamics by photoinduced electron transfer provides evidence for deviations from a regular polyproline type II helix. *Proc. Natl. Acad. Sci. U.S.A.* **2007**, *104*, 17400−17405.
(31) Owens, N. W.; Stetefeld, J.; Lattova, E.; Schweizer, F. Contiguous *O*-galactosylation of 4(*R*)-hydroxy-L-proline residues forms very stable polyproline II helices. *J. Am. Chem. Soc.* **2010**, *132*, 5036−5042.
(32) Ellis, C. R.; Maiti, B.; Noid, W. G. Specific and nonspecific effects of glycosylation. *J. Am. Soc. Chem.* **2012**, *134*, 8184−8193.
(33) Cheng, S. M.; Edwards, S. A.; Jiang, Y. D.; Grater, F. Glycosylation enhances peptide hydrophobic collapse by impairing solvation. *ChemPhysChem* **2010**, *11*, 2367−2374.
(34) Riederer, M. A.; Hinnen, A. Removal of *N*-glycosylation sites of the yeast acid-phosphatase severely affects protein folding. *J. Bacteriol.* **1991**, *173*, 3539−3546.
(35) Engelsen, S. B.; Monteiro, C.; de Penhoat, C. H.; Perez, S. The diluted aqueous solvation of carbohydrates as inferred from molecular dynamics simulations and NMR spectroscopy. *Biophys. Chem.* **2001**, *93*, 103−127.
(36) Aliev, A. E.; Courtier-Murias, D. Conformational analysis of L-prolines in water. *J. Phys. Chem. B* **2007**, *111*, 14034−14042.
(37) Park, S.; Radmer, R. J.; Klein, T. E.; Pande, V. S. A new set of molecular mechanics parameters for hydroxyproline and its use in molecular dynamics simulations of collagen-like peptides. *J. Comput. Chem.* **2005**, *26*, 1612−1616.
(38) Melis, C.; Bussi, G.; Lummis, S. C. R.; Molteni, C. Trans−cis switching mechanisms in proline analogues and their relevance for the gating of the 5-HT3 receptor. *J. Phys. Chem. B* **2009**, *113*, 12148−12153.
(39) Kang, Y. K.; Choi, H. Y. Cis−trans isomerization and puckering of proline residue. *Biophys. Chem.* **2004**, *111*, 135−142.
(40) Kang, Y. K.; Jhon, J. S.; Park, H. S. Conformational preferences of proline oligopeptides. *J. Phys. Chem. B* **2006**, *110*, 17645−17655.
(41) Venkatachalam, C. M.; Price, B. J.; Krimm, S. A theoretical estimate of the energy barriers between stable conformations of the proline dimer. *Biopolymers* **1975**, *14*, 1121−1132.
(42) Case, D. A.; Cheatham, T. E.; Darden, T.; Gohlke, H.; Luo, R.; Merz, K. M.; Onufriev, A.; Simmerling, C.; Wang, B.; Woods, R. J. The Amber biomolecular simulation programs. *J. Comput. Chem.* **2005**, *26*, 1668−1688.
(43) Case, D. A.; Darden, T. A.; T.E. Cheatham, I.; Simmerling, C. L.; Wang, J.; Duke, R. E.; Luo, R.; Crowley, M.; R. C..Walker; Zhang, W. et al. *AMBER 10*; University of California: San Francisco, 2008.
(44) Hornak, V.; Abel, R.; Okur, A.; Strockbine, B.; Roitberg, A.; Simmerling, C. Comparison of multiple AMBER force fields and development of improved protein backbone parameters. *Proteins* **2006**, *65*, 712−725.
(45) Kirschner, K. N.; Yongye, A. B.; Tschampel, S. M.; Gonzalez-Outeirino, J.; Daniels, C. R.; Foley, B. L.; Woods, R. J. GLYCAM06: A generalizable Biomolecular force field. Carbohydrates. *J. Comput. Chem.* **2008**, *29*, 622−655.
(46) Onufriev, A.; Bashford, D.; Case, D. A. Modification of the generalized Born model suitable for macromolecules. *J. Phys. Chem. B* **2000**, *104*, 3712−3720.
(47) Onufriev, A.; Bashford, D.; Case, D. A. Exploring protein native states and large-scale conformational changes with a modified generalized born model. *Proteins* **2004**, *55*, 383−394.
(48) Jorgensen, W. L.; Chandrasekhar, J.; Madura, J. D.; Impey, R. W.; Klein, M. L. Comparison of simple potential functions for simulating liquid water. *J. Chem. Phys.* **1983**, *79*, 926−935.
(49) Geyer, C. J. Markov-chain Monte Carlo maximum-likelihood. *Comput. Sci. Stat.* **1991**, 156−163.
(50) Babin, V.; Karpusenka, V.; Moradi, M.; Roland, C.; Sagui, C. Adaptively biased molecular dynamics: An umbrella sampling method with a time-dependent potential. *Int. J. Quantum Chem.* **2009**, *109*, 3666−3678.
(51) Babin, V.; Roland, C.; Sagui, C. Adaptively biased molecular dynamics for free energy calculations. *J. Chem. Phys.* **2008**, *128*, 134101.
(52) Moradi, M.; Babin, V.; Roland, C.; Darden, T. A.; Sagui, C. Conformations and free energy landscapes of polyproline peptides. *Proc. Natl. Acad. Sci. U. S. A.* **2009**, *106*, 20746−20751.
(53) Moradi, M.; Babin, V.; Sagui, C.; Roland, C. PPII Propensity of multiple-guest amino acids in a proline-rich environment. *J. Phys. Chem. B* **2011**, *115*, 8645−8656.
(54) Moradi, M.; Babin, V.; Sagui, C.; Roland, C. A statistical analysis of the PPII propensity of amino acid guests in proline-rich peptides. *Biophys. J.* **2011**, *100*, 1083−1093.
(55) Cowan, P. M.; McGavin, S. Structure of poly-L-proline. *Nature* **1955**, *176*, 501−503.
(56) Kakinoki, S.; Hirano, Y.; Oka, M. On the stability of polyproline-I and II structures of proline oligopeptides. *Polym. Bull. (Heidelberg, Ger.)* **2005**, *53*, 109−115.
(57) Gornick, F.; Mandelkern, L.; Diorio, A. F.; Roberts, D. E. Evidence for cooperative intramolecular transition in poly-L-proline. *J. Am. Soc. Chem.* **1964**, *86*, 2549−2555.
(58) Steinberg, I. Z.; Harrington, W. F.; Berger, A.; Sela, M.; Katchalski, E. The configuartional changes of poly-L-proline in solution. *J. Am. Soc. Chem.* **1960**, *82*, 5263−5279.
(59) Strassma., H.; Engel, J.; Zundel, G. Binding of alcohols to peptide co-group of poly-L-proline in I and II conformation. I. Demonstration of binding by infrared spectroscopy and optical rotatory dispersion. *Biopolymers* **1969**, *8*, 237−246.
(60) Chen, K.; Liu, Z. G.; Kallenbach, N. R. The polyproline II conformation in short alanine peptides is noncooperative. *Proc. Natl. Acad. Sci. U.S.A.* **2004**, *101*, 15352−15357.

(61) Greenfie., N.; Fasman, G. D. Computed circular dichroism spectra for evaluation of protein conformation. *Biochemistry* **1969**, *8*, 4108.
(62) Sreerama, N.; Woody, R. W. Molecular dynamics simulations of polypeptide conformations in water: A comparison of alpha, beta, and poly(Pro)II conformations. *Proteins* **1999**, *36*, 400−406.
(63) Shi, Z. S.; Olson, C. A.; Rose, G. D.; Baldwin, R. L.; Kallenbach, N. R. Polyproline II structure in a sequence of seven alanine residues. *Proc. Natl. Acad. Sci. U.S.A.* **2002**, *99*, 9190−9195.
(64) Ding, L.; Chen, K.; Santini, P. A.; Shi, Z. S.; Kallenbach, N. R. The pentapeptide GGAGG has PII conformation. *J. Am. Chem. Soc.* **2003**, *125*, 8092−8093.
(65) Avbelj, F.; Baldwin, R. L. Role of backbone solvation and electrostatics in generating preferred peptide backbone conformations: Distributions of phi. *Proc. Natl. Acad. Sci. U.S.A.* **2003**, *100*, 5742−5747.
(66) Eker, F.; Griebenow, K.; Schweitzer-Stenner, R. Stable conformations of tripeptides in aqueous solution studied by UV circular dichroism spectroscopy. *J. Am. Chem. Soc.* **2003**, *125*, 8178−8185.
(67) Eker, F.; Griebenow, K.; Cao, X. L.; Nafie, L. A.; Schweitzer-Stenner, R. Preferred peptide backbone conformations in the unfolded state revealed by the structure analysis of alanine-based (AXA) tripeptides in aqueous solution. *Proc. Natl. Acad. Sci. U.S.A.* **2004**, *101*, 10054−10059.
(68) Best, R. B.; Merchant, K. A.; Gopich, I. V.; Schuler, B.; Bax, A.; Eaton, W. A. Effect of flexibility and cis residues in single-molecule FRET studies of polyproline. *Proc. Natl. Acad. Sci. U.S.A.* **2007**, *104*, 18964−18969.
(69) Panasik, N., Jr.; Eberhardt, E. S.; Edison, A. S.; Powell, D. R.; Raines, R. T. Inductive effects on the structure of proline residues. *Int. J. Peptide Protein Res.* **1994**, *44*, 262−269.
(70) Stapley, B. J.; Creamer, T. P. A survey of left-handed polyproline II helices. *Protein Sci.* **1999**, *8*, 587−595.
(71) Tan, L.; Varnai, P.; Lamport, D. T. A.; Yuan, C. H.; Xu, J. F.; Qiu, F.; Kieliszewski, M. J. Plant *O*-hydroxyproline arabinogalactans are composed of repeating trigalactosyl subunits with short bifurcated side chains. *J. Biol. Chem.* **2010**, *285*, 24575−24583.